

Electronic Supplementary Information

Appearance of Annular Ring-like Intermediates during Amyloid Fibril Formation from Human Serum Albumin

Shruti Arya,^{a,b} Arpana Kumari,^c Vijit Dalal,^{a,c} Mily Bhattacharya,^{b,*} and Samrat
Mukhopadhyay^{a,b,c,*}

^a Centre for Protein Science Design and Engineering, ^b Department of Chemical Sciences and
^c Department of Biological Sciences, Indian Institute of Science Education and Research
(IISER), Mohali 140306, Punjab, India.

* Corresponding authors: Mily Bhattacharya and Samrat Mukhopadhyay

Email: mily@iisermohali.ac.in & mukhopadhyay@iisermohali.ac.in

Tel: +91-172-229-3150

Fax: +91-172-224-0266

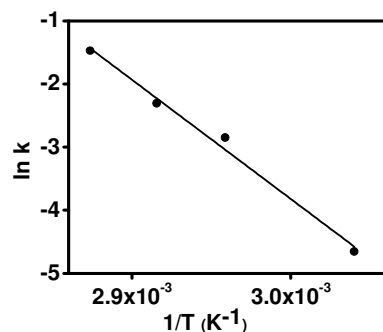


Figure S1. Arrhenius plot ($\ln k$ versus $1/T$) showing temperature dependence of HSA aggregation. The activation energy calculated from the slope of the plot was ~ 157 kJ/mol (~ 37.5 kcal/mol).

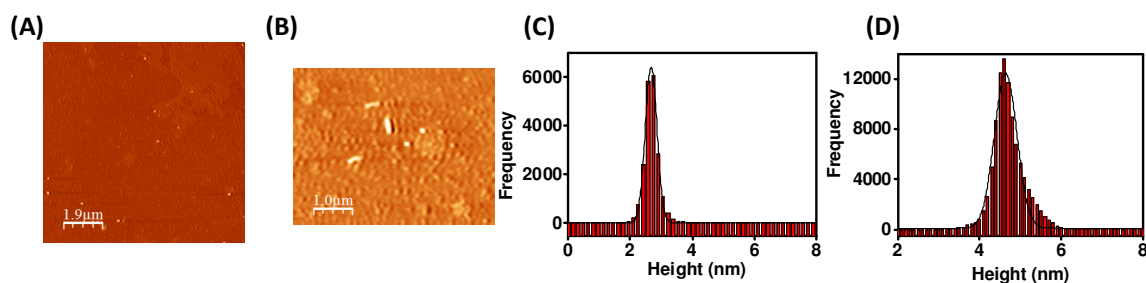


Figure S2. AFM images of (A) zero time point (0 minute) sample and (B) early oligomers/protofibrils (10 minute). The statistical height distributions of (C) zero time point (0 minute) sample and (D) oligomers (10 minute).

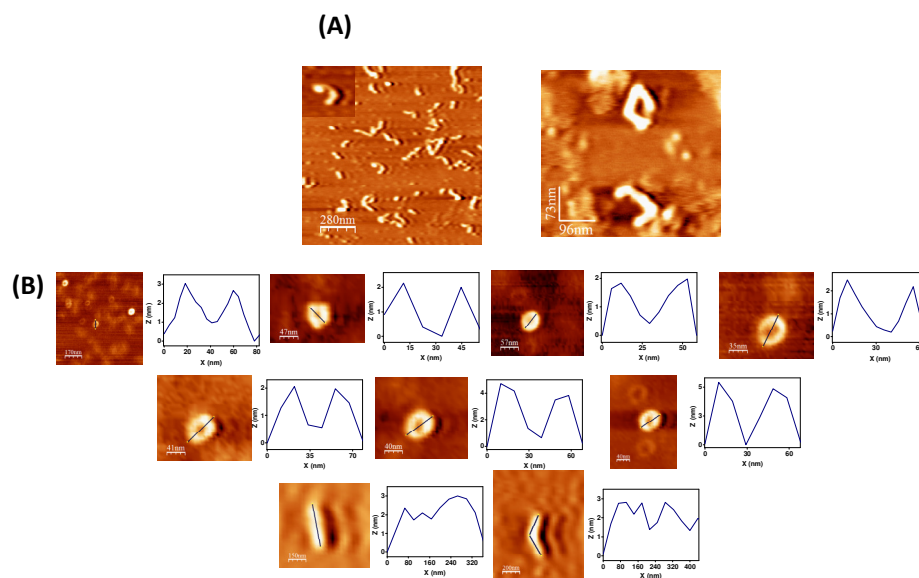


Figure S3. AFM images of (A) matured HSA fibrils formed upon prolonged incubation (for one month at room temperature) and (B) individual rings (along with their height profiles). The height profiles of the individual rings were analyzed using WSxM software.

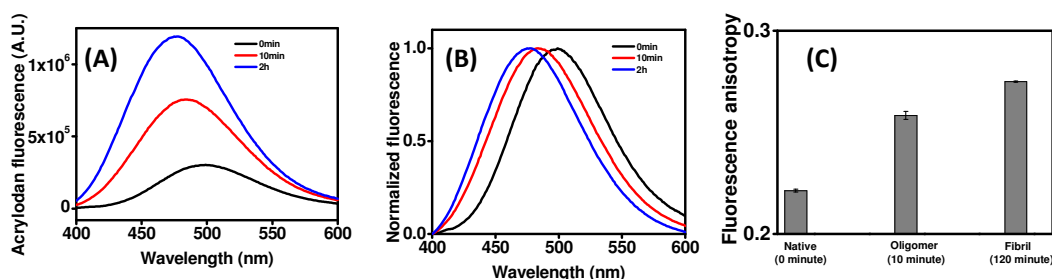


Figure S4. (A) Acrylodan (covalently attached to Cys 34) fluorescence at three different time points of aggregation. (B) Normalized fluorescence of acrylodan shows blue shift of 22 nm in the emission maximum from zero time point (0 minute) to final time point (120 minute). (C) The steady-state fluorescence anisotropy of acrylodan at three different time points.

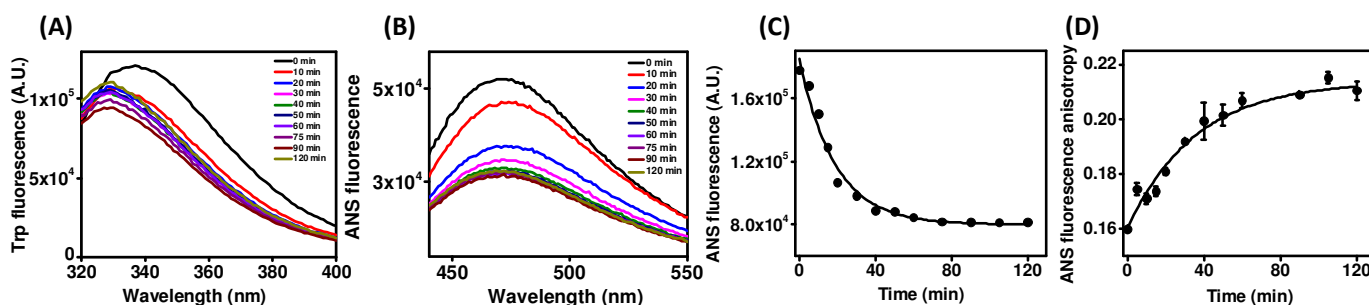


Figure S5. (A) Trp and (B) ANS fluorescence spectra at different time points of aggregation. The kinetics of amyloid formation monitored by (C) ANS fluorescence intensity, (D) ANS steady-state fluorescence anisotropy. The continuous black lines through the data points represent the fit obtained using a single-exponential equation.

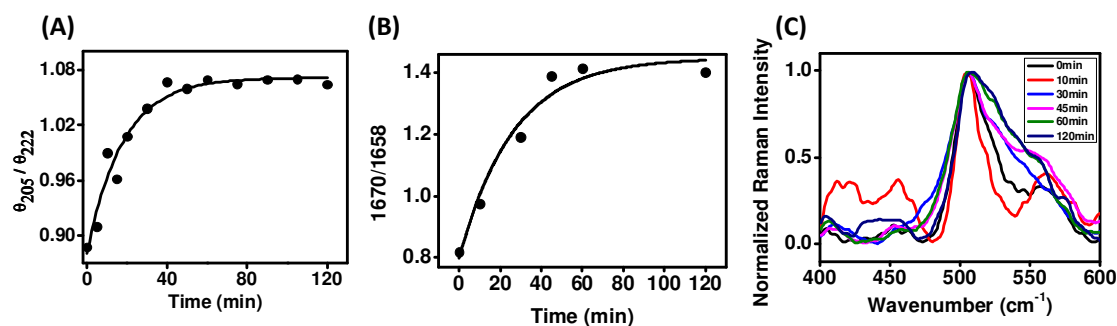


Figure S6. The kinetics of amyloid formation monitored by (A) circular dichroism (CD) and (B) Raman spectroscopy (ratio of Raman intensity at 1670 cm^{-1} to 1658 cm^{-1}). (C) Raman spectra of disulfides ($400\text{-}600 \text{ cm}^{-1}$) at different time points of HSA aggregation.

Table S1. Typical parameters (rotational correlation times, their respective amplitudes, mean fluorescence lifetimes) associated with the time-resolved fluorescence anisotropy decay of AEDANS in native (0 minute), oligomeric (10 minute) and fibrillar (120 minute) states of human serum albumin (HSA). R_h denotes the average hydrodynamic radii of HSA aggregates (estimated using Equation 7 in Experimental Methods).

Time (minutes)	ϕ_{fast} (ns) (β_{fast})	ϕ_{slow} (ns) (β_{slow})	τ_{mean} (ns)	R_h (nm)
0	0.7 (0.2)	38.5 (0.8)	15.3	3.5
10	0.7 (0.2)	58.2 (0.8)	14	4.0
120	0.6 (0.3)	> 150 (0.7)	12.2	> 6.0

Table S2. The estimated content of secondary structural elements (%) from Amide I (1620-1700 cm^{-1}) analysis using Raman spectroscopy[†]:

Time (minutes)	α -helix & coils (1645-1665 cm^{-1})	β -sheet (1665-1674 cm^{-1})	Extended conformation (1680-1690 cm^{-1})
0	77	18	3
10	74	10	11
30	48	49	10
45	37	57	5
60	39	55	5
120	37	60	8

[†] Due to the overlap of the peaks in the range of 1645-1690 cm^{-1} , there might be little overestimation of the percentage contributions associated with different secondary structure elements. However, the overall trend remains unaffected.

Table S3. The estimated content of secondary structural elements (%) from Amide III (1220-1300 cm^{-1}) analysis using Raman spectroscopy:

Time (minutes)	α-helix (1264-1300 cm^{-1})	β-sheet, coils & turns (1230-1255 cm^{-1})
0	59	41
10	43	57
30	35	65
45	18	82
60	19	81
120	5	95